

# Potential Intensity of Tropical Cyclones: Comparison of Results from Radiosonde and Reanalysis Data

MELISSA FREE

*NOAA/Air Resources Laboratory, Silver Spring, Maryland*

MARJA BISTER\*

*Meteorological Research, Finnish Meteorological Institute, Helsinki, Finland*

KERRY EMANUEL

*Program in Atmospheres, Oceans, and Climate, Massachusetts Institute of Technology, Cambridge, Massachusetts*

(Manuscript received 24 June 2003, in final form 12 November 2003)

## ABSTRACT

Long-term changes in the intensity of tropical cyclones are of considerable interest because of concern that greenhouse warming may increase storm damage. The potential intensity (PI) of tropical cyclones can be calculated from thermodynamic principles, given the state of the sea surface and atmosphere, and has been shown in earlier studies to give a reasonable estimate of maximum intensity for observed storms. The PI calculated using radiosonde data at 14 tropical island locations shows only small, statistically insignificant trends from 1980 to 1995 and from 1975 to 1995. In the mid-1990s PI at most of these stations does not show the strong increase that appears in global and regional PI calculated from reanalysis data. Comparison with results derived from reanalysis data suggests that previous adjustments to the reanalysis-derived PI may overstate PI after 1980 in some regions in comparison with that before 1980. Both reanalysis and radiosonde PI show similar interannual variability in most regions, much of which appears to be related to ENSO and other changes in SST. Between 1975 and 1980, however, while SSTs rose, PI decreased, illustrating the hazards of predicting changes in hurricane intensity from projected SST changes alone.

## 1. Introduction

Increases in hurricane intensity are expected to result from increases in sea surface temperature and decreases in tropopause-level temperature accompanying greenhouse warming (Emanuel 1987; Henderson-Sellers et al. 1998; Knutson et al. 1998). However, because the predicted increase in intensity for doubled CO<sub>2</sub> is only 5%–20%, changes over the past 50 yr would likely be less than 2%—too small to be detected easily. In fact, studies of observed frequencies and maximum intensities of tropical cyclones show no consistent upward trend (Landsea et al. 1996; Henderson-Sellers et al. 1998; Solow and Moore 2002). While actual intensity changes are hard to measure, changes in potential in-

tensity (PI) can be estimated from thermodynamic principles as shown in Emanuel (1986, 1995) given a record of SSTs and profiles of atmospheric temperature and humidity. Potential intensity is the maximum sustainable intensity of tropical cyclones based on the thermodynamic state of the atmosphere and sea surface, measured in terms of the maximum winds ( $V_{\max}$ ) or minimum central pressure ( $p_{\min}$ ). Calculations of PI agree well with the observed maximum intensities of severe tropical storms (Tonkin et al. 2000), and increases in potential intensity may affect intensity distributions of weaker tropical storms (Emanuel 2000).

Bister and Emanuel (2002a, hereafter BE02a) calculated potential intensity of tropical cyclones using data from the National Centers for Environmental Prediction–National Center for Atmospheric Research (NCEP–NCAR) reanalysis (Kalnay et al. 1996). The results after 1979 were adjusted to account for the spurious shift in reanalysis temperatures that occurred with the introduction of satellite data in the late 1970s. The adjustment was based on the comparison of PI for years before and after 1979 with similar SSTs. As BE02a noted, this adjustment is subject to considerable uncer-

\* Current affiliation: Department of Physical Sciences, University of Helsinki, Helsinki, Finland.

Corresponding author address: Dr. Melissa Free, NOAA/Air Resources Laboratory, SSMC3, Room 3151, 1315 East West Highway, Silver Spring, MD 20910.  
E-mail: melissa.free@noaa.gov

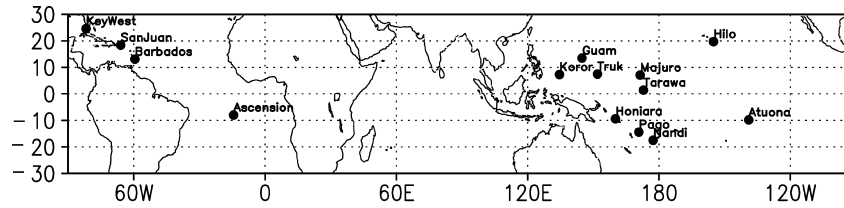


FIG. 1. Locations of stations used.

tainty, making the results unsuitable for trend analysis before 1980. Other possible errors in the NCEP–NCAR reanalysis, discussed in detail in BE02a, may also affect the calculated potential intensities.

In this paper we calculate potential intensity using radiosonde and SST data and compare the resulting seasonal cycles and annual mean time series to those from BE02a at grid points near selected radiosonde stations. Because the radiosonde data do not have any major discontinuity in the late 1970s, this allows a more confident assessment of changes in PI at these locations before and after 1980. We also explore the reasons for interannual changes in our calculated PI.

## 2. Methods

We calculated potential intensity by the method described in Emanuel (1995) and BE02a, using the relation

$$V_{\max}^2 = \frac{T_s}{T_0} - \frac{C_k}{C_D} (\text{CAPE}^* - \text{CAPE})_m, \quad (1)$$

where  $T_s$  is the SST,  $T_0$  is the mean outflow temperature (temperature at the level of neutral buoyancy),  $C_k$  is the exchange coefficient for enthalpy,  $C_D$  is a drag coefficient,  $\text{CAPE}^*$  is the convective available potential energy of air

lifted from saturation at sea level in reference to the environmental sounding, and  $\text{CAPE}$  is that of boundary layer air.  $\text{CAPE}^*$  and  $\text{CAPE}$  are evaluated at the radius of maximum wind of the hypothetical cyclone using a reversible adiabatic parcel-lifting algorithm. To get the pressure at the radius of maximum wind, which is needed for the  $\text{CAPE}$  calculation, we use the relation

$$c_p T_s \ln(p_0/p_m) = 0.5V_{\max}^2 + \text{CAPE}_m, \quad (2)$$

where  $p_0$  is the ambient surface pressure and  $p_m$  is the pressure at the radius of maximum wind (see BE02a). Equations (1) and (2) are solved iteratively.

The calculated  $V_{\max}$  is reduced by 10% to account for the difference between gradient winds and winds near the surface. The calculation is done for each day with sufficient data, but only days for which the calculated  $V_{\max}$  exceeds  $40 \text{ m s}^{-1}$  are included in the means. Monthly means are calculated only if PI results exist and exceed this threshold for at least 10 days in the month. The minimum central pressure ( $p_{\min}$ ) is obtained from  $V_{\max}$  by a relation similar to Eq. (2).

To minimize spurious trends from changes in sounding resolution over time, we interpolated the radiosonde soundings to 10-mb resolution and to the 13 levels used by BE02a. Results using the 10-mb resolution are generally a few meters per second larger than those using only 13 levels. The lowest level used, representing the boundary layer, was 1000 mb, except at Guam, where 990 mb was used because 1000 mb was not consistently above the surface. Statistical significance of trends is determined by comparison to the uncertainty (twice the standard error of the trend) with degrees of freedom adjusted to account for autocorrelation using the formula  $n_{\text{eff}} = n(1 - r)/(1 + r)$ , where  $r$  is the lag-1 autocorrelation of the time series.

## 3. Data

We selected 14 island radiosonde stations in the Tropics (see Fig. 1 and Table 1) having relatively long and complete records. For the calculation of potential intensity, daily temperature data from the troposphere up to 70 mb and humidity data from the lower troposphere are necessary. We used soundings from the Comprehensive Aerological Reference Data Set (Eskridge et al. 1995) and monthly mean SSTs from NCEP EOF analyses (Smith et al. 1996). Many stations suitable for stud-

TABLE 1. Names, WMO identification numbers, and locations of radiosonde stations used, along with the number of missing months from 1975 to 1995. A dash indicates that too few data points exist at the particular time to be used.

Station	WMO no.	Months missing		Lat	Lon
		0000 UTC	1200 UTC		
Truk	91334	2	—	7.5	151.9
Nandi	91680	6	—	−17.5	177.3
Pago Pago	91765	1	7	−14.4	170.8
Hilo	91285	16	10	19.7	−155.1
Guam	91217	10	23	13.5	144.8
San Juan	78526	2	1	18.4	−66.0
Key West	72201	5	2	24.6	−81.8
Barbados	78954	71	26	13.1	−59.5
Ascension Island	61902	—	82	−8.0	−14.4
Koror	91408	2	—	7.3	134.5
Tarawa	91610	79	—	1.4	172.9
Atuona	91925	43	—	−9.8	139.0
Honiara	91517	96	—	−9.4	160.1
Majuro	91376	2	—	7.1	171.4

ies of lower-tropospheric trends could not be used here because of sparse data near the tropopause.

Homogeneity was assessed using station histories from the National Climatic Data Center (NCDC) and visual inspection of time series of temperature and humidity at 1000 mb and temperature at 70 mb, as well as the PI results (PI calculations are not sensitive to humidity in the upper troposphere). Where both day and night observations exist, we examine also time series of the day–night differences of these quantities. If a sudden, sustained level shift in temperature or humidity coincided with a similar discontinuity in PI, and the changes did not appear to be explained by known large-scale natural variations, such as ENSO or volcanic eruptions, the station was considered inhomogeneous at that time. Because of widespread changes in humidity sensors before 1974 (Gaffen 1996), we considered only results after that date. At seven stations (the first seven listed in Table 1) the results are considered homogeneous between 1975 and 1995 at a minimum. At the other seven stations, discontinuities in temperature or humidity time series between these dates, which do not appear to be natural, make the results unreliable for trend calculations. Despite these inhomogeneities, these stations are useful for the investigation of climatology and interannual variability.

#### 4. Results

Figure 2 shows seasonal cycles of minimum central pressure ( $p_{\min}$ ) for the 14 stations, grouped by location. This plot shows only results from daytime soundings. At Guam and Hilo, Hawaii, intensities are greater ( $p_{\min}$  is lower) for night soundings than day soundings, but at San Juan, Puerto Rico, Key West, Florida, Barbados, and Pago Pago, the two observation times give very similar results. As expected, the amplitude of the seasonal cycle in the Caribbean stations increases with distance from the equator. In the Pacific, however, this relationship is less evident, with Atuona showing a larger seasonal cycle than other stations, despite its greater proximity to the equator. In the Northern Hemisphere, maximum intensities (minimum pressures) generally occur in September or October and minimum intensities (maximum pressures) in late winter. Koror and Tarawa show a more complex pattern, with maxima in May and December at Koror, and in February and November at Tarawa. In the Southern Hemisphere, minima occur in or near August and maxima are between December and March. Honiara, with higher SSTs than the other stations, shows much greater intensities, with central pressures below 850 mb for 5 months of the year. Intensities at Ascension Island and Hilo are less than at the other stations. These features are generally consistent with the results based on reanalysis data described in Bister and Emanuel (2002b). The  $p_{\min}$  at Honiara, Solomon Islands, is about 20-mb lower than in BE02a, while Tarawa  $p_{\min}$

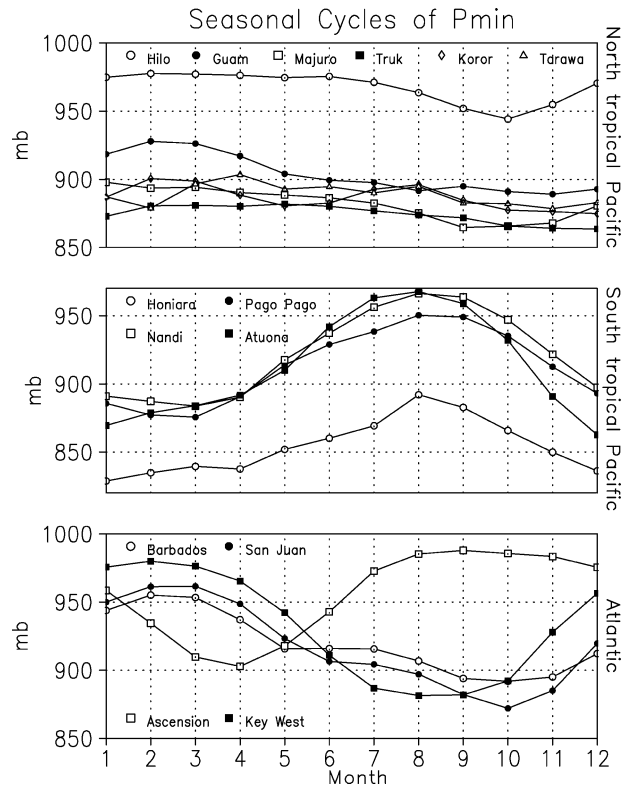


FIG. 2. Seasonal cycles of potential intensity at 14 radiosonde stations expressed as minimum central pressure (mb), calculated from data for 1982–95, grouped by geographic region. Plots show daytime results only.

is higher than in Bister and Emanuel (2002b) by a similar amount.

Figure 3 compares annual means of  $V_{\max}$  from radiosonde data at seven homogeneous stations to those from reanalysis data at grid boxes at the same locations from BE02a. It also shows the Southern Oscillation index (SOI) for comparison. Interannual variability in the PI series is generally anticorrelated with ENSO (positively correlated with the SOI), especially in the western Pacific. Correlations between PI and the SOI range from 0.052 at Hilo to 0.70 at Pago Pago, with all but Hilo and San Juan significantly correlated. Before 1980, mean PIs are generally similar in both datasets, but after 1980 the BE02a results are higher than radiosonde results by a few meters per second at many stations. Nandi, Hilo, San Juan, and Key West are exceptions, showing little relative shift in PI between 1978 and 1980. At several of these stations, a relative shift in PI between the radiosonde and reanalysis results occurs in 1976/77, several years before the adjustment in reanalysis PI.

Our results generally show similar interannual variability to that from BE02a after 1980. Barbados and San Juan are exceptions, with less agreement in year-to-year variability between the two sets of results. The two homogeneous locations in the Caribbean (Key West and San Juan) show less upward trend in reanalysis PI than

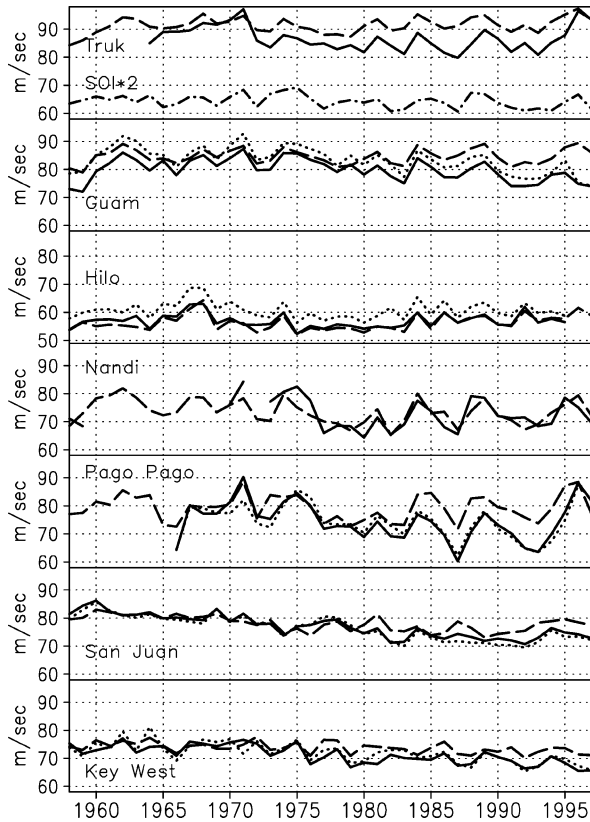


FIG. 3. Annual mean PI expressed as maximum wind speed ( $\text{m s}^{-1}$ ) for seven stations from radiosonde day (solid lines), night (dotted lines), and reanalysis (dashed lines) data, with (top) the Southern Oscillation index (dash-dotted line, multiplied by 2). (PI from radiosonde data is sometimes discontinuous due to data gaps.)

the larger-scale North Atlantic mean shown in BE02a, suggesting that these locations may not be representative.

Table 2 shows the correlations between PIs in the sonde and reanalysis results for the 14 stations. Almost all of the correlations, which range from 0.27 to 0.95, are significant at the 95% level. Correlations are generally higher for 1980–95 than for 1973–97.

Table 3 shows the trends for the reanalysis and radiosonde  $V_{\max}$  for the individual stations for 1980–95, none of which is significant at the 95% level. For 1975–95 (not shown) Guam and Pago Pago have significant negative trends and Hilo has a significant positive trend in the radiosonde data, while reanalysis has significant positive trends at Tarawa and Majuro, Marshall Islands.

The mean of the PIs for the homogeneous stations in the northwest tropical Pacific, southwest tropical Pacific, and Caribbean, along with the mean for the 7 most homogeneous radiosonde stations together and for all 14 stations, is compared to the equivalent mean PI from BE02a in Fig. 4. The two sets of time series are very similar in interannual variability between 1980 and 1995, but the reanalysis-based PI in the northwest and southwest Pacific shows an upward jump relative to the

TABLE 2. Correlations between annual mean  $V_{\max}$  from radiosonde and from reanalysis (BE02a) by station. Correlations in boldface are significant at the 95% level.

Station name	Correlation 1973–97	Correlation 1980–95
Truk	<b>0.73</b>	<b>0.82</b>
Nandi	<b>0.72</b>	<b>0.78</b>
Pago Pago*	<b>0.73</b>	<b>0.84</b>
Pago Pago**	<b>0.61</b>	<b>0.70</b>
Hilo*	<b>0.95</b>	<b>0.93</b>
Hilo**	<b>0.87</b>	<b>0.83</b>
Guam*	<b>0.43</b>	<b>0.89</b>
Guam**	0.34	<b>0.88</b>
San Juan*	<b>0.46</b>	<b>0.62</b>
San Juan**	0.35	<b>0.72</b>
Key West*	<b>0.77</b>	<b>0.69</b>
Key West**	<b>0.70</b>	<b>0.53</b>
Barbados*	<b>0.55</b>	0.55
Barbados**	<b>0.59</b>	<b>0.61</b>
Ascension*	<b>0.60</b>	<b>0.55</b>
Koror	0.42	0.27
Tarawa	<b>0.62</b>	<b>0.82</b>
Atuona	<b>0.47</b>	<b>0.63</b>
Honiara	<b>0.52</b>	<b>0.71</b>
Majuro	<b>0.59</b>	<b>0.64</b>

\* 0000 UTC.

\*\* 1200 UTC.

sonde-based result in 1980, presumably because of the adjustment of the reanalysis PI by BE02a. This effect is not clearly evident in the Caribbean.

Table 4 shows trends in the regional and overall means for 1980–95 and 1975–95 for both reanalysis and radiosonde results. From 1980 on, the majority of

TABLE 3. Linear least squares trends in  $V_{\max}$  from the annual time series ( $\text{m s}^{-1} \text{ decade}^{-1}$ ) by station. Uncertainty column is 2 times the standard error.

Station name	Trend—sondes		Trend—reanalysis	
	1980–95	$\pm$	1980–95	$\pm$
Truk	0.75	3.1	0.30	2.4
Nandi	3.41	5.3	0.64	4.3
Pago Pago*	−0.61	6.5	2.72	5.8
Pago Pago**	−3.71	6.7		
Hilo*	1.79	1.9	2.69	2.0
Hilo**	0.70	1.8		
Guam*	−2.04	3.9	−0.06	3.4
Guam**	−2.70	4.3		
San Juan*	−1.01	2.7	0.13	3.4
San Juan**	−0.30	2.2		
Key West*	−2.14	3.0	−0.86	1.5
Key West**	−0.67	1.9		
Barbados*	2.22	3.6	0.50	4.4
Barbados**	0.80	3.4		
Ascension*	3.28	5.4	1.03	2.2
Koror	3.23	2.8	1.15	2.4
Tarawa	2.96	5.3	4.82	6.1
Atuona	−3.49	8.9	0.30	4.7
Honiara	3.71	5.1	3.99	3.5
Majuro	2.58	5.3	1.99	3.0

\* 0000 UTC.

\*\* 1200 UTC.

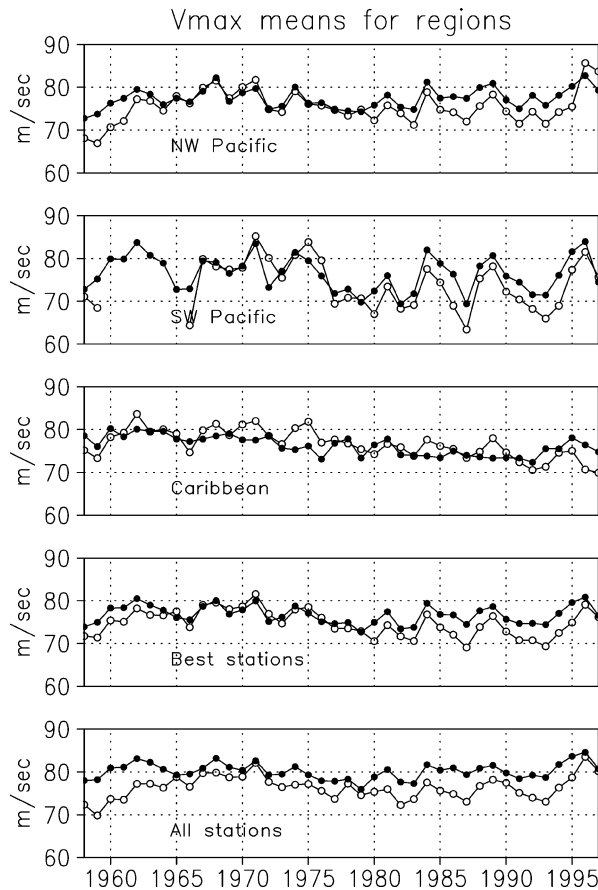


FIG. 4. Regional and global annual means of PI ( $\text{m s}^{-1}$ ) from radiosonde (open circles) and reanalysis (closed circles) data. "NW Pacific" includes Truk, Guam, and Hilo. "SW Pacific" includes Pago Pago and Nandi. "Caribbean" includes San Juan and Key West. "Best stations" is the mean of the seven stations considered homogeneous from at least 1974–95: Truk, Guam, Hilo, San Juan, Key West, Pago Pago, and Nandi.

trends are positive, but none is statistically significant at the 95% level. (None exceeds the 95% confidence interval of twice the standard error, which is adjusted for autocorrelation of the time series). For 1975–95, a negative trend in the Caribbean in the sonde results and positive trend in the northwest tropical Pacific in the reanalysis results are barely significant. Trends in the reanalysis results for these groups of stations are generally slightly larger than for radiosondes after 1980, and at least  $1 \text{ m s}^{-1} \text{ decade}^{-1}$  larger than sonde results for the longer time period. These differences are not statistically significant.

## 5. Discussion

Because model studies predict only a 3–7  $\text{m s}^{-1}$  increase in tropical cyclone intensity with a doubling of  $\text{CO}_2$  (e.g., Emanuel 1987; Knutson et al. 1998; Henderson-Sellers et al. 1998) associated with a 2.2-K increase in SST, the lack of a detectable upward trend in

TABLE 4. Trends in regional mean potential intensity ( $\text{m s}^{-1} \text{ decade}^{-1}$ ). Uncertainty column is 2 times the standard error.

	Radiosonde trend	Uncertainty	Reanalysis trend	Uncertainty
1980–95 trend				
Best stations	−0.17	2.6	0.79	2.2
All stations	1.07	2.6	1.38	2.2
Northwest Pacific	−0.13	2.0	0.98	2.1
Southwest Pacific	0.62	5.2	1.68	5.0
Caribbean	−1.90	3.0	0.21	2.0
1975–95 trend				
Best stations	−1.50	2.1	0.92	1.5
All stations	0.34	1.5	1.66	1.7
Northwest Pacific	−0.47	1.3	1.62	1.8
Southwest Pacific	−2.09	4.4	1.18	3.5
Caribbean	−2.60	2.1	0.92	1.3

PI since the mid 1970s is not surprising. The general similarity in interannual variability between the radiosonde and reanalysis PI suggests that the intradecadal changes shown in both time series may be real. However, although we avoid the problem of discontinuity at 1979 present in the reanalysis data, using radiosonde data allows only a very limited sampling of the tropical atmosphere. Because the sonde data are weighted heavily toward the northwestern tropical Pacific, and do not sample the Pacific east of  $140^\circ\text{W}$  at all, they may tend to understate any changes related to ENSO variability. The results shown here may, therefore, not be representative of the Tropics as a whole. In particular, the relative jump upward of the reanalysis results in comparison with the radiosonde results in 1979/80 appears to be larger in the western Pacific than elsewhere in the Tropics, so that the overall effect of the adjustments made in BE02a is likely to be less than that shown at these locations.

Apart from the adjustment made to PI by BE02a, differences between our radiosonde-based results and those of BE02a for the same locations can arise from differences in SSTs or in the sounding temperatures and humidities. The SSTs are in most cases almost identical, but the monthly means of soundings can differ noticeably between radiosondes and the reanalysis. Such differences may arise from undetected inhomogeneities in the radiosonde soundings, inhomogeneities in the reanalysis due to problems with the radiosonde or satellite inputs, or unrealistic effects of the reanalysis model. Inhomogeneities that produce spurious drying (see Ross and Gaffen 1998) or cooling would tend to give unrealistic increases in PI. Also, our results for specific locations may not correspond well to results for larger regions due to our limited spatial sampling.

In most time periods, PI tends to be positively correlated with SST changes. From 1975 to 1980, however, PI decreases strongly while SST rises in the seven-station mean and regional mean plots. Specific humidity and temperature increase noticeably in the radiosonde data over this period at the seven best stations (see Fig.

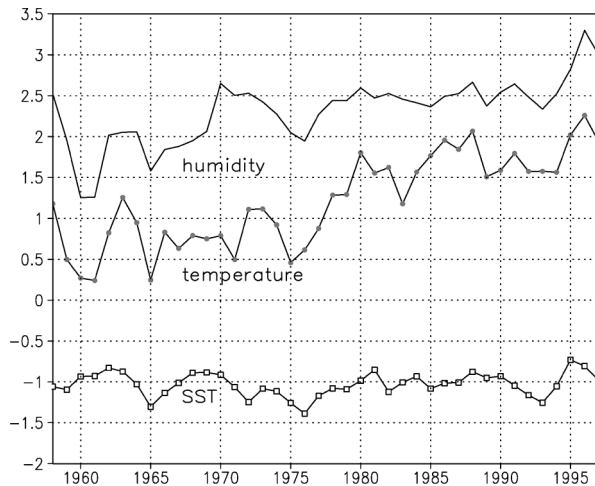


FIG. 5. Anomalies of specific humidity ( $\text{g kg}^{-1}$ ) and temperature (K) at 1000 mb from radiosonde data and SST (K) for the seven best stations. Curves have been shifted vertically to facilitate comparison.

5). Ross and Elliott (2001) saw a similar increase at many tropical stations. Such increases in boundary layer humidity (and, to a much lesser extent, temperature) tend to decrease the potential intensity in the calculation used here (see BE02a, Table 2). The result of the competing influences of increasing SST and increasing boundary layer humidity is in this case a decrease in PI. Thus, SST changes alone do not account for all changes in PI.

## 6. Conclusions

Our results show no significant trend in potential intensity from 1980 to 1995 and no consistent trend from 1975 to 1995. This result is consistent with the lack of long-term trend in observed intensities and with the relatively small size of expected changes, but differs from the upward tendency seen in regional and global means of reanalysis-based PI in BE02a. The adjustment made in BE02a to account for discontinuities in the reanalysis time series may overstate PI after 1980 in comparison with that before 1980 in some regions. Seasonal cycles are similar in radiosonde-based and reanalysis-based PI. Both BE02a and radiosonde PI show similar interannual variability in most cases, much of which appears to be related to ENSO and other changes in SST. Because the calculated PI is reduced with increasing boundary layer

temperature and humidity, increases in SST are not always associated with increases in PI.

*Acknowledgments.* We thank Dian Seidel for helpful discussions and comments on the manuscript. Roger Smith and an anonymous reviewer provided comments that improved the paper.

## REFERENCES

- Bister, M., and K. Emanuel, 2002a: Low frequency variability of tropical cyclone potential intensity. 1. Interannual to interdecadal variability. *J. Geophys. Res.*, **107**, 4801, doi:10.1029/2001JD000776.
- , and —, 2002b: Low frequency variability of tropical cyclone potential intensity. 2. Climatology from 1982–1995. *J. Geophys. Res.*, **107**, 4621, doi:10.1029/2001JD000780.
- Emanuel, K. A., 1986: An air–sea interaction theory for tropical cyclones. Part I: Steady-state maintenance. *J. Atmos. Sci.*, **43**, 585–604.
- , 1987: The dependence of hurricane intensity on climate. *Nature*, **326**, 483–485.
- , 1995: Sensitivity of tropical cyclones to surface exchange coefficients and a revised steady-state model incorporating eye dynamics. *J. Atmos. Sci.*, **52**, 3969–3976.
- , 2000: A statistical analysis of tropical cyclone intensity. *Mon. Wea. Rev.*, **128**, 1139–1152.
- Eskridge, R. E., O. A. Alduchov, I. V. Chernykh, P. Zhai, A. C. Polansky, and S. R. Doty, 1995: A Comprehensive Aerological Reference Data Set (CARDS): Rough and systematic errors. *Bull. Amer. Meteor. Soc.*, **76**, 1759–1776.
- Gaffen, D. J., 1996: A digitized metadata set of global upper-air station histories. NOAA Tech. Memo. ERL ARL-198, 162 pp.
- Henderson-Sellers, A., and Coauthors, 1998: Tropical cyclones and global climate change: A post-IPCC assessment. *Bull. Amer. Meteor. Soc.*, **79**, 19–38.
- Kalnay, E., and Coauthors, 1996: The NCEP/NCAR 40-Year Reanalysis Project. *Bull. Amer. Meteor. Soc.*, **77**, 437–471.
- Knutson, T., R. Tuleya, and Y. Kurihara, 1998: Simulated increase of hurricane intensities in a  $\text{CO}_2$ -warmed climate. *Science*, **279**, 1018–1020.
- Landsea, C., N. Nicholls, W. Gray, and L. Avila, 1996: Downward trends in the frequency of intense Atlantic hurricanes during the past five decades. *Geophys. Res. Lett.*, **23**, 1697–1700.
- Ross, R. J., and D. J. Gaffen, 1998: Comment on “Widespread tropical atmospheric drying from 1979 to 1995” by Steven R. Schroeder and James P. McGuirk. *Geophys. Res. Lett.*, **25**, 4357–4358.
- , and W. P. Elliott, 2001: Radiosonde-based Northern Hemisphere tropospheric water vapor trends. *J. Climate*, **14**, 1602–1612.
- Smith, T. M., R. W. Reynolds, and R. E. Livezey, 1996: Reconstruction of historical sea surface temperatures using empirical orthogonal functions. *J. Climate*, **9**, 1403–1420.
- Solow, A. R., and L. J. Moore, 2002: Testing for trend in North Atlantic hurricane activity, 1900–98. *J. Climate*, **15**, 3111–3114.
- Tonkin, H., G. J. Holland, N. Holbrook, and A. Henderson-Sellers, 2000: An evaluation of thermodynamic estimates of climatological maximum potential tropical cyclone intensity. *Mon. Wea. Rev.*, **128**, 746–762.